Published in final edited form as:
Mol Cancer Ther. 2008 July ; 7(7): 2233–2240. doi:10.1158/1535-7163.MCT-08-0067.

Effect of antigen turnover rate and expression level on antibody penetration into tumor spheroids

Margaret E. Ackerman[1], **David Pawlowski**[4], and **K. Dane Wittrup**[2,3]

[1]Department of Biology, Massachusetts Institute of Technology, Cambridge, Massachusetts

[2]Department of Biological Engineering, Massachusetts Institute of Technology, Cambridge, Massachusetts

[3]Department of Chemical Engineering, Massachusetts Institute of Technology, Cambridge, Massachusetts

[4]Department of Electrical Engineering and Computer Science, Case Western Reserve University, Cleveland, Ohio

Abstract

Poor tissue penetration is a significant obstacle to the development of successful antibody drugs for immunotherapy of solid tumors, and diverse alterations to the properties of antibody drugs have been made to improve penetration and homogeneity of exposure. However, in addition to properties of the antibody drug, mathematical models of antibody transport predict that the antigen expression level and turnover rate significantly influence penetration. As intrinsic antigen properties are likely to be difficult to modify, they may set inherent limits to penetration. Accordingly, in this study, we assess their contribution by evaluating the distance to which antibodies penetrate spheroids when these antigen properties are systematically varied. Additionally, the penetration profiles of antibodies against carcinoembryonic antigen and A33, two targets of clinical interest, are compared. The results agree well with the quantitative predictions of the model and show that localizing antibody to distal regions of tumors is best achieved by selecting slowly internalized targets that are not expressed above the level necessary for recruiting a toxic dose of therapeutic. Each antibody-bound antigen molecule that is turned over or present in excess incurs a real cost in terms of penetration depth—a limiting factor in the development of effective therapies for treating solid tumors.

Introduction

Antibody therapeutics promise highly specific tumor targeting. However, their superior molecular recognition characteristics have not proved to be the magical bullet once hoped. This is partly due to difficulty in obtaining sufficiently uniform exposure, particularly in solid tumors. For example, radioimmunotherapy has achieved relative success in treating blood cancers, such as lymphoma, where it is emerging as a promising front-line treatment but more limited success against solid tumors (1). These discrepant results are reflective of the additional obstacles to delivering drugs to solid tissue, where efficient delivery depends on the interplay of several unfavorable transport rates (2,3). Particularly significant rate processes include the

Requests for reprints: K. Dane Wittrup, Massachusetts Institute of Technology Building E19-551, 77 Massachusetts Avenue, Cambridge, MA 02139. Phone: 617-253-4578; Fax: 617-253-1954. wittrup@mit.edu.

Disclosure of Potential Conflicts of Interest
No potential conflicts of interest were disclosed.

rate of antibody escape from the vasculature and the ability of the therapeutic to penetrate tissue (4).

Antibodies have very low rates of extravasation, making transport across the vasculature a considerable barrier. For directly conjugated antibody therapeutics, the resulting concentration profile, where the blood often contains a 100-fold to 1,000-fold higher concentration of therapeutic than surrounding tissue (4-6), obviously limits efficacy. When combined with a long circulatory half-life, the elevated blood concentration often results in bone marrow toxicity before therapeutic toxicity throughout a solid tumor is reached.

Once out of the vasculature, there are further obstructions to tumor permeation by antibody drugs. The specific architecture of solid tumors, such as limited convective flow, high interstitial pressure, and a dense extracellular matrix, acts to limit penetration (3). The well-studied impediment of the “binding site barrier” (7,8) results from the intersection of the slow diffusion and fast association rates of high affinity antibodies. The combined effect of these rates is that binding sites closest to the vasculature are occupied before further penetration occurs. This phenomenon results in a highly heterogeneous distribution of drug-with areas of saturation surrounding the blood supply and a complete lack of antibody in more distal regions (9). Depending on the mode of cell killing, such a heterogeneous distribution can be highly undesirable.

To evade these barriers to penetration, numerous alterations have been made to the composition of the protein drug itself (1). Decreased size increases both extravasation and diffusivity (10, 11), whereas albumin binding domains (9,12) and interactions with FcRn (13,14) have been engineered to lengthen plasma residence time and allow more therapeutic to extravasate before clearance. Low affinity binders have been shown to circumvent the binding site barrier and allow a more homogeneous distribution of therapeutic (8) at the unacceptable cost, however, of significantly reducing the amount of antibody retained in the tumor.

Despite these efforts, solid tumor penetration remains an elusive goal. To account for the various processes affecting penetration, the simplified scaling model of Thurber et al. (4) describes the relevant kinetic rates and processes determining penetration in spherical micrometastases and vascularized tumors. For the purposes of the present experiments with spheroids, the relationships for micrometastases will be tested. Rearrangement of the Thiele modulus, a dimensionless group describing the ratio of catabolism to transport, yields an expression predicting the distance (R) that a prevascular spheroidal metastasis will be penetrated by an antibody (Eq. A).

$$R = \sqrt{\frac{D[\mathrm{Ab}]_{\mathrm{surface}}}{k_e([\mathrm{Ag}]_{\mathrm{tumor}}/\varepsilon)}} \qquad \text{(A)}$$

Whereas many of the variables in this expression relate to the properties of the antibody, such as the dose ($[\mathrm{Ab}]_{\mathrm{surface}}$), void fraction ($\varepsilon$), and diffusivity ($D$), the remaining terms describe antigen properties which could set intrinsic limits to penetration. These terms include the antigen expression level ($[\mathrm{Ag}]_{\mathrm{tumor}}$) and turnover rate ($k_e$). Intuitively, it is clear how each of these variables could limit the penetration of a high affinity therapeutic: the distance each antibody can penetrate before binding depends on the density of binding sites; and as bound antigen is turned over and replaced, new binding sites are exposed. In fact, if turnover occurs on a timescale comparable with vascular escape and diffusion, the result is a bottomless sink for therapeutic and a limit to further tissue penetration.

Accordingly, we experimentally varied antigen concentration and turnover rate to probe their importance in tissue penetration. Quantitative determinations of the radius of penetration were achieved by incubating tumor spheroids in fluorescent antibodies against carcinoembryonic antigen (CEA) and A33. These antigen-specific properties have been less well investigated than those of the therapeutic protein itself, despite the fact that under some conditions they may pose an intrinsic limit to tumor penetration. Identification of the antigen properties that significantly affect tumor penetration will aid in the selection of targets with favorable profiles and in optimizing this promising mode of cancer therapy.

Materials and Methods

Cell and Spheroid Culture

LS174T and SW1222 cells were cultured as described previously (16). Antigen expression levels were quantified using Quantum Simply Cellular Beads (Bangs Laboratories, Inc.). Spheroids were grown by the hanging drop method (17). Briefly, ~500 cells were suspended in 20 μL of media in each well of a 72-microwell plate (Nunc 448698) and incubated upside-down at 37°C and 5% CO_2 for 2 to 3 d. Spheroids were then transferred to glass coverslip-bottomed dishes (Lab-Tek 155411) and allowed to adhere for 2 d before imaging. Except where noted, antibodies were added to culture media after this transfer, and the spheroids at each condition were then imaged repeatedly over time. Care was taken to ensure that antibody binding did not result in depletion from the bulk.

Fluorescent Antibodies

The mouse anti-A33 antibody m100.310 was conjugated with Alexa*488 according to the manufacturer's instructions (Molecular Probes A-20181) with an average of 2.7 fluorophores per antibody. Anti-CEA IgGs M85151a and M111147 were purchased from Fitzgerald and likewise conjugated with Alexa*488, with resulting conjugation levels of 1.5 and 1.4 fluorophores per antibody, respectively, for experiments comparing penetration distance with respect to internalization rate and 2.1 fluorophores per molecule of antibody M85151a for all other CEA experiments presented.

Image Collection and Analysis

A Zeiss LSM 510 confocal microscope with a 1.4 NA air lens at 10× magnification on a heated stage was used to collect spheroid images. Image collection conditions were optimized for each antibody used and then maintained for all time points in each experiment. Care was taken to analyze images at an appropriate depth from the coverslip to avoid both artifacts based on incomplete adhesion to the coverslip and attenuation of signal due to the thickness of the sample. Images were transferred to ImageJ, in which they were despeckled and gated to eliminate background signal, yielding a binary image. A circular selection area was then drawn around each spheroid, and the macro “spheroidspin” was run (see supplementary data for macro code).[5] This protocol draws a line across the selection and gives a pixel-by-pixel readout of signal intensity on that line as the image is rotated in 18 projections, each varying by 20°, and generates a results table listing the readout for each line, the sum of pixels with signal for each projection, and the average number of pixels with signal across projections. This average gives the diameter of the spheroid that has been penetrated by fluorescent antibody in pixels, which are then converted into microns. The penetration distances reported here are the averages of 3 to 10 spheroids under each condition and therefore represent a total of 90 to 360 individual measurements of penetration radius. Error bars represent the SD of the penetration distance

[5]Supplementary material for this article is available at Molecular Cancer Therapeutics Online (http://mct.aacrjournals.org/).

between spheroids. However, at later time points and higher concentrations of antibody, the spheroids become completely saturated and the SD reflects variability in spheroid size.

Results

Spheroids—spherical clusters of growing, self-adhered tumor cells—were used extensively in this study as a model system intermediate between monolayer tissue culture and xenografts to capture the effects of simultaneous diffusion, binding, and endocytic uptake. Spheroids present a three-dimensional environment in which cells grow without any solid or artificial support. At large sizes, spheroids also recapitulate phenomena of tumors, such as hypoxic and necrotic cores (18). Lacking any blood or lymph-driven convective flow, they provide a reasonable model for transport within the center of a bulk vascularized tumor (19). After an initial period of growth, they may be analyzed by either two-photon or confocal microscopy or fixed and handled as a histologic specimen.

In this study, spheroids were grown in a hanging drop (17), allowed to adhere to coverslips, incubated in the presence of various fluorescently labeled antibodies, and imaged by confocal microscopy. Raw images (Fig. 1A) were analyzed to determine the average distance that antibody penetrated into the spheroid at a given time. After acquisition, images were gated to generate a binary version (Fig. 1B), such that background signal was excluded. A circular region of interest was drawn around each spheroid, and pixel-by-pixel intensity was taken along a bisecting diagonal line as the region of interest was rotated in 18 projections around 360° (Fig. 1C). The number of pixels above the selected intensity threshold was summed and then averaged over all projections, giving the diameter of the spheroid that had been penetrated by label. The macro for this analysis may be found in the supplementary materials.[5]

Equation A predicts that penetration distance, R, will increase proportionally to $[Ab]_{surface}$ and inversely proportional to $[Ag]_{tumor}$. Accordingly, a 10-fold decrease in antigen density is expected to yield a 10-fold increase in penetration distance. Similarly, the model also predicts that a 10-fold decrease in antigen density will negate the effect of a 10-fold decrease in antibody dose.

To experimentally test these predictions, spheroids were incubated in either a given concentration of fluorescent anti-A33 antibody or a mixture of fluorescent antibody and nonfluorescent competitor. The nonfluorescent competitor functions to occupy a fraction of binding sites, as both antibodies diffuse through the spheroid, blocking the fluorescent antibody from binding and allowing it to diffuse further into the spheroid before encountering an available binding site. Accordingly, the nonfluorescent competitor acts as a means to effectively tune the density of available antigen binding sites.

When spheroids were incubated in either a given concentration of fluorescent anti-A33 antibody or a mixture of one-tenth that concentration of fluorescent and nine-tenths nonfluorescent competitor antibody, penetration was indeed equivalent (Fig. 2A)—as would be expected given that the total antibody dose is equivalent in both cases. The decrease in fluorescent antibody dose worsens the signal to noise ratio; however, the equivalence of total dose leads to equivalent penetration distance, as can be seen in representative images at 24 hours (Fig. 2B and C).

For a given dose of fluorescent antibody, penetration distance is predicted to vary proportionally to $[Ag]_{tumor}$. Therefore, when available $[Ag]_{tumor}$ is decreased 10-fold due to the presence of unlabeled competitor, the model predicts that the penetration distance will increase by a factor of 10—close to the value observed at a concentration of 0.15 nmol/L at 24 hours (Fig. 2D, *black columns*). At higher concentrations (*gray columns*) and later time points, this ratio decreases to 1, as the spheroids become completely saturated to their centers under

both conditions (error bars represent the variation in spheroid size). As predicted theoretically (4, 5) and shown experimentally previously (20), increasing antibody dose is one route to overcoming the binding site barrier.

To explore the dependence on antigen density by an independent method, spheroids were grown from cell lines expressing different levels of antigen. SW1222 cells express one-fifth as much A33 antigen as LS174T cells (data not shown). This 5-fold decrease in antigen density is predicted to lead to a 5 increase in penetration distance. As can be seen at 12 hours, 1.5 nmol/L antibody almost completely penetrates the SW1222 spheroid while advancing only a few cell layers in an LS174T spheroid (Fig. 3A versus B). The relative distance that the antibody front penetrates in each spheroid cell type was quantified and is given over a range of concentrations at 12 hours (Fig. 3C). When these penetration distances are taken as a ratio, they agree well with the model prediction (Fig. 3D).

To study the effect of internalization rate on penetration, we used antibodies against CEA that exhibit differing internalization rates. Despite binding to the same cellular target, M85151a and M111147 display an ~3-fold difference in internalization rate.[6] This difference is likely related to antibody M85151a's recognition of two epitopes per CEA molecule, allowing cross-linking of the antigen. When the increased internalization rate of M85151a and a 2-fold increase in binding sites are incorporated into the model, M111147 is predicted to penetrate into spheroids 2.3-fold further than M85151a. Indeed, when LS174T spheroids were incubated with each of these antibodies, there were clear differences in penetration. The more quickly internalizing M85151a ($t_{1/2}$, 5 hours) clearly penetrates the spheroid to a lesser extent than M111147 ($t_{1/2}$, 13 hours). Figure 4A and B are representative sections of spheroids labeled with M85151a and MS111147, respectively. To quantitatively compare the difference in penetration, the ratio of the penetration distances of slow to fast internalizing antibodies was taken at various concentrations (Fig. 4C). Here again, at early times and low concentrations, before spheroids become saturated and the ratio approaches unity, the data were found to agree well with the model prediction of a 2.3-fold difference.

Thus, both antigen turnover and antigen density have significant effects on tumor penetration and should be considered in the selection of targets. Whereas a high antigen density is beneficial for increasing the exposure of each cell to the therapeutic, excessively high density inhibits penetration and increases heterogeneity. Likewise, antigen turnover results in continual replenishment of available binding sites and can thereby act as a bottomless sink for therapeutic and block further tissue penetration. Figure 5 compares two alternative antigens. Both A33 and CEA are present at similar expression levels in LS174T cells and each has a long history of study as a target in radioimmunotherapy of colon cancer (21-25). However, CEA has a metabolic turnover halflife of 15 hours,[5] whereas the halflife of A33 stretches out to almost 60 hours (16). Even the seemingly slow internalization rate of CEA has a significant effect on tumor penetration. Figure 5A and B present the distance penetrated by various antibody doses over time. A 150 nmol/L concentration of anti-CEA antibody has saturated the spheroid by the first time point, at 6 hours. Therefore, at this concentration, the increase in the penetration distance beyond that at 6 hours is due to growth of the spheroid, and this line represents the maximum penetration distance achievable. At low concentrations, penetration arrests when antibody diffusion comes to steady-state with antigen turnover (Fig. 5A). This arrest is evident as a stalled fluorescence front, which can be observed in 24-hour and 48-hour images of cells exposed to 1.5 nmol/L anti-CEA antibody (Fig. 5C, *top*). As a result, at this concentration of therapeutic, cells at the center of the spheroid will never be exposed.

[6]M.M. Schmidt, G.M. Thurber, K.D. Wittrup. Kinetics of anti-carcinoembryonic antigen antibody internalization: effects of affinity, bivalency, and stability. Cancer Immunol Immunother. 2008; April 12 [Epub ahead of print].

In contrast, the slower internalization rate of A33 not only allows 1.5 nmol/L antibody (Fig. 3C, *center*) to continue to progress toward the center, but even 0.07 nmol/L doses (*bottom*) continue to progress and reach the spheroid center eventually. Significantly, antibodies to A33 have been shown to accomplish penetration to the core of tumors *in vivo* in clinical trials (21, 22)—an unusual result for an IgG. We hypothesize that the slow rate of antigen turnover contributes significantly to this highly desirable attribute.

Therapeutic strategies, such as pretargeted radioimmunotherapy, antibody-directed enzyme prodrug therapy, and antibody-dependent cellular cytotoxicity, rely on sustained accessibility of the tumor-bound therapeutic to a second agent and are therefore negatively effected by internalization. As a means to study the effect of internalization and turnover on the surface accessibility of antibody over time, spheroids were grown in antibody, washed, incubated in fresh media, and imaged daily to follow the fate of bound antibody. Over the period of observation, fluorescent signal may decrease due to antibody internalization and degradation or unbinding and diffusion out of the spheroid or, in the case of CEA, when antigen is shed. As in previous experiments, spheroids continue to grow over the period of observation. Therefore, fluorescence is also diluted via the division of labeled cells. Figure 6A shows the observed patterns of staining over the course of 4 days after removal of label. A33 and CEA show dramatically different staining patterns: A33 antibody remains relatively evenly distributed throughout the spheroid, whereas CEA exhibits a punctuate localization pattern.

To visualize the amount of antibody that remained surface localized 4 days after removal of the antibody from culture media, spheroids were incubated with a secondary antibody (anti-mouse PE conjugate), washed, and imaged (Fig. 6B). Strikingly, much of the anti-A33 antibody remains surface-localized and accessible to secondary, while with the exception of a few punctuate regions, accessible anti-CEA antibody is largely absent. Considering the secondary labeling antibody as a proxy for the second agent in any multistep targeting strategy, such as PRIT or antibody-directed enzyme prodrug therapy, Fig. 6B illustrates a marked preference for A33 as a target.

Discussion

The limited tissue penetration of antibody drugs is an obstacle to successful solid tumor immunotherapy and has led to diverse efforts to increase tumor exposure (1). A variety of drug level optimizations have been pursued, including increasing diffusivity and extravasation, extending plasma halflife, and lowering affinity—each aimed to increase penetration and improve the homogeneity of solid tumor exposure. Similarly, tumor microenvironment has been manipulated to favor better penetration. Various investigators have studied the effect of altering the extracellular matrix, vascular transport, and interstitial pressure and transport variables, often via combination therapy (15,26-30). Clearly, there is widespread recognition that a good penetration profile is critical to therapeutic success and consequently much effort has been put into optimizing tumor exposure—both by manipulating drug properties and the tumor microenvironment.

However, less attention has been paid to the properties of the target antigen that might pose intrinsic limits to penetration. Previous theory predicts that both the expression level and turnover rate of the antigen can affect penetration (4,5). This study provides experimental evidence that under some circumstances antigen properties can be the determining factor in tumor penetration and supports the selection of antigens with slower turnover and lower expression.

As this report shows, antigen density can have a dramatic effect on tumor penetration. Of course, the greater penetration observed with lower antigen density is in direct opposition to

the practice of selecting highly expressed tumor antigens to increase the amount of drug to which each cell is exposed. And, somewhat ironically, to the extent that expression level has been manipulated in targeting, it has been to up-regulate expression via IFN-γ treatment (27), which, as shown here, would be predicted to decrease overall penetration depths.

Similarly, the data presented in this study has significant implications for the models used in the study of immunotherapy. Such models have often used cell lines that grossly overexpress the target antigen or have been modified in ways that can affect turnover, such as by transfection. Accordingly, the resulting distribution of drug in such models may be highly artifactual. To accurately capture antibody distribution, accurate recapitulation of antigen properties is required.

In practice, once an antigen is expressed at levels sufficient to recruit a lethal dose of therapeutic, additional antigen counterproductively leads to poorer tumor penetration and a more heterogeneous dosing of the tumor. Because the level of expression sufficient to induce cytotoxicity may vary widely depending on the mode of therapy used, bounds for optimal antigen expression levels will be case specific. Highly potent toxic modalities, such as a emitters or some protein toxins, may be best suited for low antigen expression, whereas other less potent therapeutics may require high expression to be effective. Likewise, for some modes of toxicity, such as therapies using radionuclides with long deposition distances, complete penetration may be unnecessary as untargeted cells can accumulate a toxic dose via crossfire or other local environment effects. Nonetheless, regardless of the expression level required for cytotoxic effect, incremental expression above that level incurs a cost in terms of reduced penetration.

We have also shown that turnover can set an inherent limit to penetration: if the target is replaced at a rate similar to the diffusion of the therapeutic through tissue, complete penetration may be impossible. Here too, however, the preferred antigen turnover rate will depend on the mechanism of cell killing, because internalization is critical to immunotoxin and antibody-drug conjugate therapies, for example. Slow turnover remains desirable for penetration, but internalization is necessary for efficacy in such cases—leaving the goals of reaching distal cells and high drug activity in direct opposition. In contrast, two-step therapies, such as antibody-directed enzyme prodrug therapy, pretargeted radioimmunotherapy, or effector function rely on persistent surface localization and antibody/antigen turnover acts to directly decrease cell killing. Because altering a single variable can have multiple and even competing effects, it is instructive to look to quantitative, predictive models to assess such tradeoffs when designing therapies. The complexity of relationships between transport, binding, and other kinetic processes can lead to nonintuitive outcomes, which are captured by a properly formulated model.

The data presented here underscore the reality that tumor-specific expression is truly only the first criteria that a target antigen must meet. Depending on its other properties, use of certain modes of therapy may be highly inadvisable. Therefore, selection from among the repertoire of toxic mechanisms should take into account the properties of the target antigen. Differences between A33 and CEA, the two targets used in this study, highlight the importance of such target-tailored therapy design. The more rapid turnover of CEA has multiple implications. First, a greater dose of therapeutic is required to achieve equivalent penetration. Secondly, as time passes, progressively less targeting drug remains surface localized and able to bind a second agent in a two-step therapy. Conversely, more molecules of immunotoxin would be internalized during a given period of time, likely making CEA the preferred target for immunotoxin therapy, relative to A33.

In contrast, the relative stability of A33 is especially promising for two-step therapies. Observations made here as to the ability of antibodies to A33 to penetrate spheroids at even extremely low doses are paralleled by experience in the clinic, where even the necrotic centers of tumors are labeled (21,22) and where antibody is detectable a month and a half after administration. This stable profile would allow for both improved dosing of distal cells, as well as the recruitment of the toxic effector at a level similar to antigen expression. The fact that clinically observed differences between the penetration of antibodies against A33 relative to other targets are reproduced here suggests both that the spheroids used here are a reasonably representative model of *in vivo* tumors and that antigen properties are indeed relevant to clinical biodistribution results.

Whereas antibody therapeutics have well-demonstrated difficulty in penetrating tissue, this difficulty is generally ascribed to their large size. However, there is a significant body of literature describing the inability of even small molecule drugs to penetrate tissue. Clearly, if even orders of magnitude changes in size, extravasation, and diffusivity cannot lead to thorough tumor penetration, there are other variables that must have a considerable effect on distribution and penetration. Minchinton and Tannock provide an excellent review of the distribution of small molecules in tumors as a factor in therapeutic outcome (2). Many of the factors cited to influence antibody penetration also figure prominently for small molecules, and it is likely that the target properties explored here can play a similar role in determining the distribution and efficacy of small molecules.

Overall, the data presented here quantitatively validate the model of Thurber et al. (4) and show the importance of antigen-specific variables in tumor penetration. As tissue penetration is a significant hurdle in the success of therapeutics, care must be taken not only to optimize the properties of the drug itself to maximize penetration, but also in the selection of target antigen. Dosing of distal regions of tumors is best achieved by selecting highly stable targets that are not expressed above the level necessary for recruitment of a toxic dose of therapeutic. Whereas a high antigen density is beneficial for increasing the exposure of each cell to the therapeutic, excessively high density inhibits penetration and increases heterogeneity. Likewise, antigen turnover results in continual replenishment of available binding sites and can thereby act to inhibit further tissue penetration. Each molecule of antigen that is either turned over or present in excess incurs a real cost in terms of penetration—a significant obstacle to the development of effective immunotherapies for solid tumors.

Supplementary Material

Refer to Web version on PubMed Central for supplementary material.

Acknowledgments

We thank the Ludwig Institute for providing antibodies and cell lines.

Grant support: National Cancer Institute grant CA101830.

References

1. Beckman RA, Weiner LM, Davis HM. Antibody constructs in cancer therapy: protein engineering strategies to improve exposure in solid tumors. Cancer 2007;109:170–9. [PubMed: 17154393]
2. Minchinton AI, Tannock IF. Drug penetration in solid tumours. Nat Rev Cancer 2006;6:583–92. [PubMed: 16862189]
3. Jain RK. Transport of molecules, particles, and cells in solid tumors. Annu Rev Biomed Eng 1999;1:241–63. [PubMed: 11701489]

4. Thurber GM, Zajic SC, Wittrup KD. Theoretic criteria for antibody penetration into solid tumors and micrometastases. J Nucl Med 2007;48:995–9. [PubMed: 17504872]
5. Graff CP, Wittrup KD. Theoretical analysis of antibody targeting of tumor spheroids: importance of dosage for penetration, and affinity for retention. Cancer Res 2003;63:1288–96. [PubMed: 12649189]
6. Thurber GM, Schmidt MM, Wittrup KD. Antibody tumor penetration: transport opposed by systemic and antigen-mediated clearance. Adv Drug Deliv Rev. 2007 In press.
7. van Osdol W, Fujimori K, Weinstein JN. An analysis of monoclonal antibody distribution in microscopic tumor nodules: consequences of a “binding site barrier.”. Cancer Res 1991;51:4776–84. [PubMed: 1893370]
8. Adams GP, Schier R, McCall AM, et al. High affinity restricts the localization and tumor penetration of single-chain fv antibody molecules. Cancer Res 2001;61:4750–5. [PubMed: 11406547]
9. Dennis MS, Jin H, Dugger D, et al. Imaging tumors with an albumin-binding Fab, a novel tumor-targeting agent. Cancer Res 2007;67:254–61. [PubMed: 17210705]
10. Covell DG, Barbet J, Holton OD, Black CD, Parker RJ, Weinstein JN. Pharmacokinetics of monoclonal immunoglobulin G1, F(ab′)2, and Fab′ in mice. Cancer Res 1986;46:3969–78. [PubMed: 3731067]
11. Colcher D, Pavlinkova G, Beresford G, Booth BJ, Choudhury A, Batra SK. Pharmacokinetics and biodistribution of genetically-engineered antibodies. Q J Nucl Med 1998;42:225–41. [PubMed: 9973838]
12. Dennis MS, Zhang M, Meng YG, et al. Albumin binding as a general strategy for improving the pharmacokinetics of proteins. J Biol Chem 2002;277:35035–43. [PubMed: 12119302]
13. Kenanova V, Olafsen T, Crow DM, et al. Tailoring the pharmacokinetics and positron emission tomography imaging properties of anti-carcinoembryonic antigen single-chain Fv-Fc antibody fragments. Cancer Res 2005;65:622–31. [PubMed: 15695407]
14. Ghetie V, Popov S, Borvak J, et al. Increasing the serum persistence of an IgG fragment by random mutagenesis. Nat Biotechnol 1997;15:637–40. [PubMed: 9219265]
15. Netti PA, Hamberg LM, Babich JW, et al. Enhancement of fluid filtration across tumor vessels: implication for delivery of macromolecules. Proc Natl Acad Sci U S A 1999;96:3137–42. [PubMed: 10077650]
16. Ackerman ME, Chalouni C, Raman VV, et al. A33 antigen displays persistent surface expression. Cancer Immunol Immunother 2008;57:1017–27. [PubMed: 18236042]
17. Kelm JM, Timmins NE, Brown CJ, Fussenegger M, Nielsen LK. Method for generation of homogeneous multicellular tumor spheroids applicable to a wide variety of cell types. Biotechnol Bioeng 2003;83:173–80. [PubMed: 12768623]
18. Sutherland RM, Durand RE. Radiation response ofmulticell spheroidsan *in vitro* tumour model. Curr Top Radiat Res Q 1976;11:87–139. [PubMed: 128440]
19. Pluen A, Boucher Y, Ramanujan S, et al. Role of tumor-host interactions in interstitial diffusion of macromolecules: cranial vs. subcutaneous tumors. Proc Natl Acad Sci U S A 2001;98:4628–33. [PubMed: 11274375]
20. Saga T, Neumann RD, Heya T, et al. Targeting cancer micro-metastases with monoclonal antibodies: a binding-site barrier. Proc Natl Acad Sci U S A 1995;92:8999–9003. [PubMed: 7568060]
21. Welt S, Divgi CR, Real FX, et al. Quantitative analysis of antibody localization in human metastatic colon cancer: a phase I study of monoclonal antibody A33. J Clin Oncol 1990;8:1894–906. [PubMed: 2230877]
22. Scott AM, Lee FT, Jones R, et al. A phase I trial of humanized monoclonal antibody A33 in patients with colorectal carcinoma: biodistribution, pharmacokinetics, and quantitative tumor uptake. Clin Cancer Res 2005;11:4810–7. [PubMed: 16000578]
23. Liersch T, Meller J, Bittrich M, Kulle B, Becker H, Goldenberg DM. Update of carcinoembryonic antigen radioimmunotherapy with (131)ilabetuzumab after salvage resection of colorectal liver metastases: comparison of outcome to a contemporaneous control group. Ann Surg Oncol 2007;14:2577–90. [PubMed: 17570017]
24. Goldenberg DM, Gaffar SA, Bennett SJ, Beach JL. Experimental radioimmunotherapy of a xenografted human colonic tumor (GW-39) producing carcinoembryonic antigen. Cancer Res 1981;41:4354–60. [PubMed: 7306964]

25. Begent RH, Verhaar MJ, Chester KA, et al. Clinical evidence of efficient tumor targeting based on single-chain Fv antibody selected from a combinatorial library. Nat Med 1996;2:979–84. [PubMed: 8782454]

26. Jang SH, Wientjes MG, Au JL. Enhancement of paclitaxel delivery to solid tumors by apoptosis-inducing pretreatment: effect of treatment schedule. J Pharmacol Exp Ther 2001;296:1035–42. [PubMed: 11181938]

27. Brouwers AH, Frielink C, Oosterwijk E, Oyen WJ, Corstens FH, Boerman OC. Interferons can upregulate the expression of the tumor associated antigen G250-MN/CA IX, a potential target for (radio)immunotherapy of renal cell carcinoma. Cancer Biother Radiopharm 2003;18:539–47. [PubMed: 14503948]

28. Jain RK. Antiangiogenic therapy for cancer: current and emerging concepts. Oncology (Huntingt) 2005;19:7–16. [PubMed: 15934498]

29. Mok W, Boucher Y, Jain RK. Matrix metalloproteinases-1 and -8 improve the distribution and efficacy of an oncolytic virus. Cancer Res 2007;67:10664–8. [PubMed: 18006807]

30. McKee TD, Grandi P, Mok W, et al. Degradation of fibrillar collagen in a human melanoma xenograft improves the efficacy of an oncolytic herpes simplex virus vector. Cancer Res 2006;66:2509–13. [PubMed: 16510565]

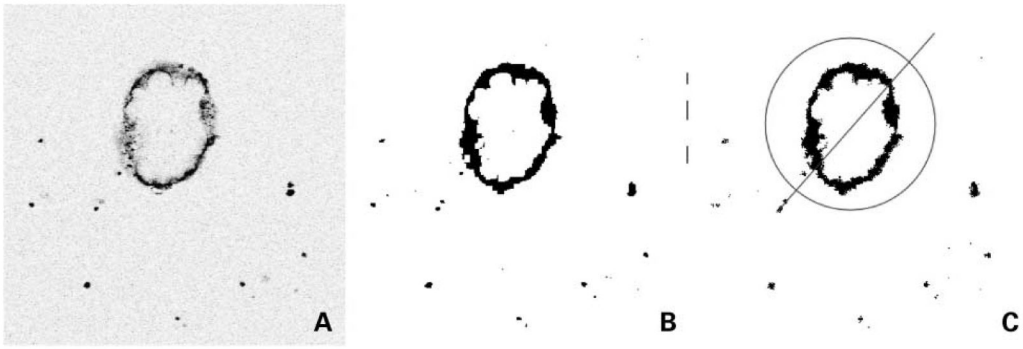

Figure 1.

Processing of spheroid images. **A**, original confocal images were transferred into ImageJ. **B**, they were then processed to eliminate background signal and generate binary data. **C**, a circular region of interest was drawn around each spheroid, and a readout of pixel intensity along a bisecting diagonal line was taken as the image was rotated in 18 projections around 360°. The number ofpixels with signal from each projection was then averaged, yielding the diameter of the spheroid that had been penetrated by label.

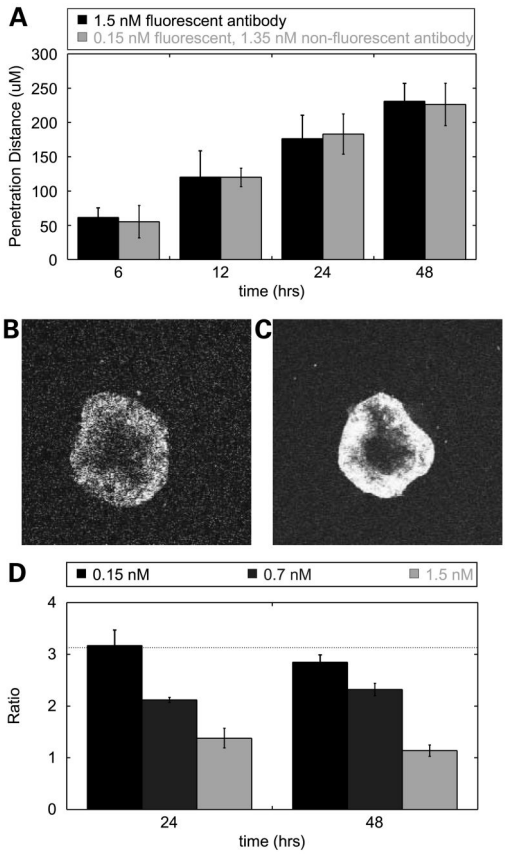

Figure 2.

Antigen density affects spheroid penetration. **A**, LS174T spheroids were labeled with 1.5 nmol/L fluorescent A33 antibody (*black*) or 0.15 nmol/L fluorescent and 1.35 nmol/L nonfluorescent competitor (*gray*). The penetration distance ofthe fluorescent antibody into spheroids under each condition was highly correlated over time. **B** and **C**, representative image of an LS174T spheroid at 24 h labeled with 0.15 nmol/L fluorescent and 1.35 nmol/L nonfluorescent competitor (**B**) or 1.5 nmol/L fluorescent antibody (**C**). **D**, ratio of penetration for spheroids with differing numbers of available binding sites (1:10) at 0.15, 0.7, and 1.5 nmol/L doses of fluorescent antibody at 24 and 48 h. The penetration ratio is a maximum of 3.2 at the lowest concentration, very close to the predicted value of 10 (*horizontal line*). Over time and at greater concentrations, this ratio approaches a value of 1 as the spheroids become saturated, setting an upper limit on the penetration distance.

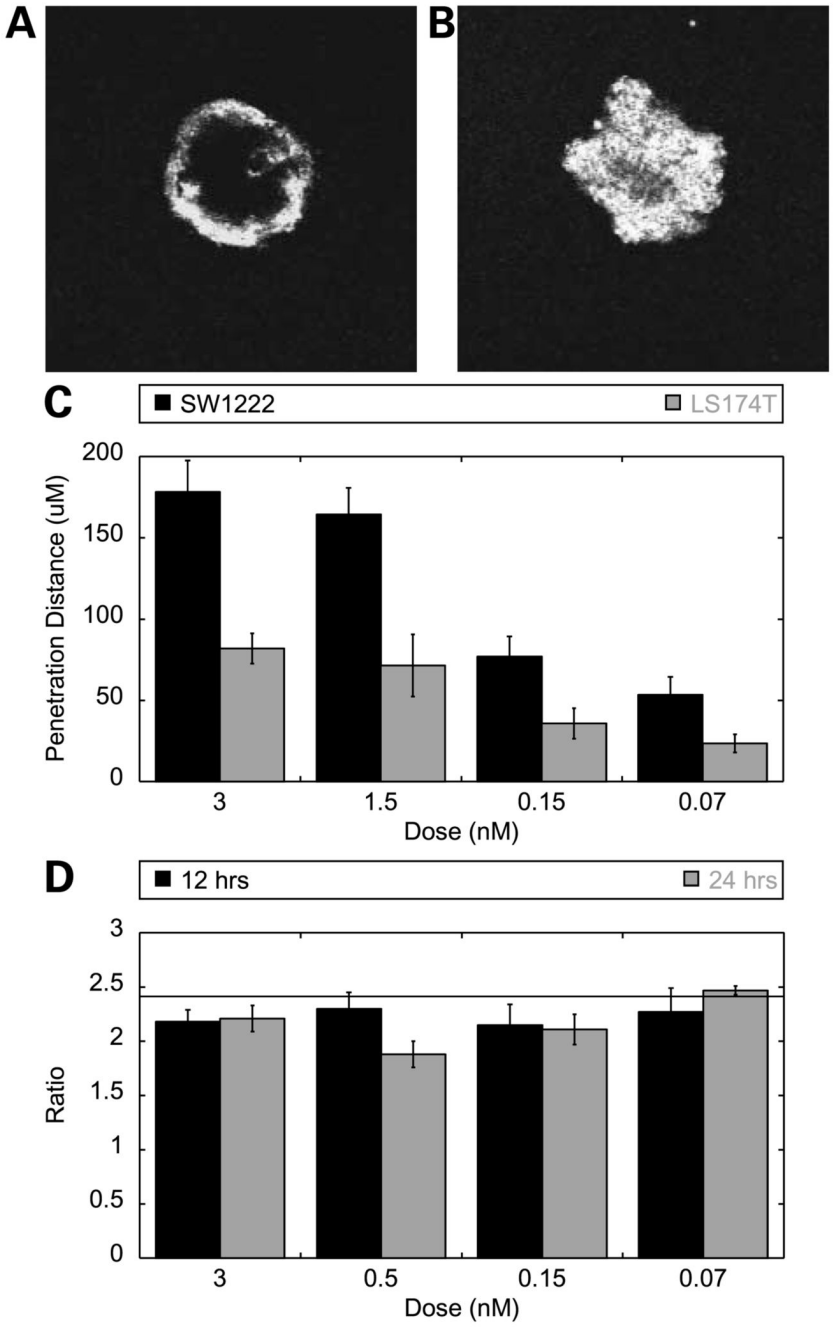

Figure 3.

Antigen density affects spheroid penetration. **A** and **B**, representative images of an LS174T (**A**) and SW1222 (**B**) spheroids labeled with 1 nmol/L A33 antibody at 12 h. **C**, penetration distance into SW1222 (*black*) and LS174T (*gray*) spheroids at 12 h. **D**, ratio of penetration (SW1222/LS174T) at 12 (*black*) and 24 (*gray*) h and the predicted value of 2.45 (*horizontal line*).

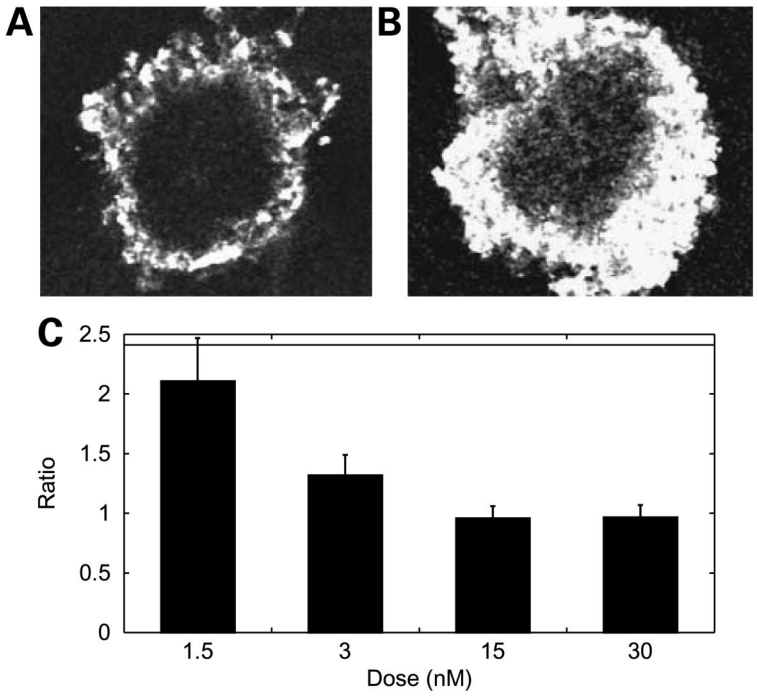

Figure 4.

Antigen internalization and turnover affects penetration. **A** and **B**, representative images ofLS174T spheroids labeled with 1.5 nmol/L CEA antibody M85151a (**A**) or M111147 (**B**). **C**, ratio of penetration depth (slow M111147/fast M85151a) over a range of concentrations at 48 h compared with the predicted value of 2.3. At greater concentrations, this ratio damps out to a value of 1 as the spheroids become saturated, setting an upper limit on the penetration distance.

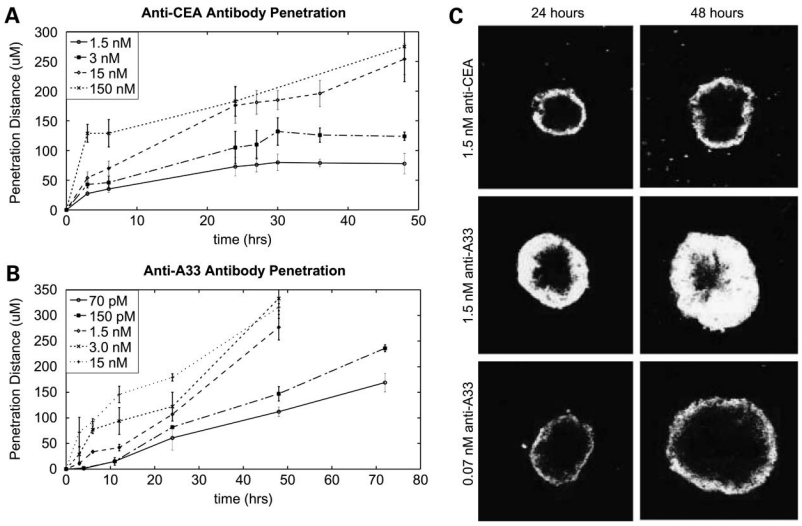

Figure 5.

Antigen internalization reaches a steady-state with diffusion and can limit penetration. Penetration of anti-CEA (**A**) and anti-A33 (**B**) antibodies into LS174T spheroids. At low concentrations, anti-CEA antibody penetration plateaus at a given radius, whereas antibodies to A33 accomplish penetration at much lower concentrations. **C,** representative images of spheroids at 24 (*left*) and 48 (*right*) h with 1.5 nmol/L anti-CEA antibody (*top*), 1.5 nmol/L anti-A33 antibody (*middle*), and 0.07 nmol/L anti-A33 antibody. After 24 h, antibody to CEA does not penetrate further into the spheroid mass, despite elapsed time.

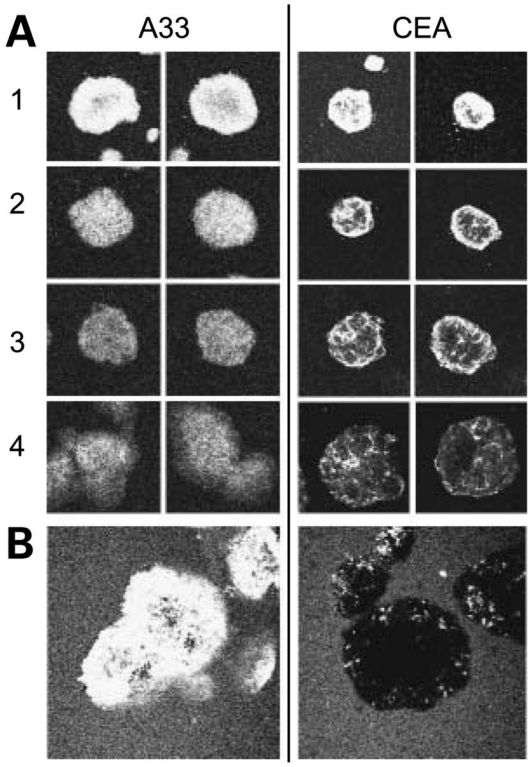

Figure 6.
Differential in-spheroid turnover and accessibility of A33 and CEA antibody over time. **A,** images of LS174T spheroids grown in A33 (*left*) or CEA (*right*) antibody. Antibody was then removed from the bulk, and spheroids were imaged 1 to 4 d postremoval to follow the localization and persistence offluorescent antibody. **B,** 4 d after label was washed out, spheroids were labeled with an antimouse antibody conjugated with PE, allowing identification of the surface accessible primary antibody.